Journal of Materials Science: Materials in Electronics (2018) 29:9494–9508
https://doi.org/10.1007/s10854-018-8983-6

Synthesis, characterization and properties of polystyrene/NiO nanocomposites

Esmaiel Soleimani[1] · **Mostafa Mohammadi**[1]

Received: 22 January 2018 / Accepted: 21 March 2018 / Published online: 26 March 2018

Abstract
In this study, polystyrene (PSt)/NiO nanocomposites (NCs) were prepared in three stages. First, NiO_2 was prepared by the reaction of $Ni(NO_3)_2{\cdot}6H_2O$ with sodium hypochlorite in the present of CTAB in alkaline solution, and then its oxidation by ethanol, obtained NiO nanoparticles (NPs). Second, the surface of NiO NPs was modified in order to obtain better dispersity and proper compatibility in organic media by oleic acid. Surface modification of NiO NPs was confirmed through lipophilic degree (LD). The results revealed that LD increased with the rising amount of modifier up to 5 wt%. Optimum modification was obtained at 65 °C and 4 h for reaction time. Third, the modified NiO NPs were dispersed in styrene monomer, and PSt/NiO NCs were synthesized via miniemulsion polymerization. The NiO NPs, its modified NPs and PSt/NiO NCs were characterized by XRD, FT-IR, FE-SEM, EDX, XPS and VSM. The average crystallite sizes of NiO were calculated to be 14 nm from XRD patterns. The results of EDX analysis and FT-IR spectra showed that chains of oleic acid have been successfully grafted on surface of NiO NPs. The morphological observation revealed that NiO NPs were embedded homogeneously in the inner part of polystyrene. Thermal stability of PSt/NiO NCs was studied using techniques of TGA and DSC. Compared to polystyrene, PSt/NiO NCs prepared by this method increased the glass transition temperature to 29 °C and increased the thermal degradation temperature that to 45 °C. The VSM results showed that the NiO NPs and PSt/NiO NCs have super paramagnetic properties.

1 Introduction

Despite the desirability of composite technology, in most cases, composite materials have not responded to industrial needs. In recent years, researchers have found that joints that create small-size materials with surrounding phases are far more powerful than larger ones. Based on this, nanocomposite science has been developed [1].

The need for increased fuel has raised the demand for lightweight materials such as polymers. However, due to the low strength of the polymers, reinforcing the polymer with the addition of quantitative (less than 10% by weight) of NPs seems to be necessary; provided it does not damage the two distinct characteristics of the polymer (the style and ease of processability). Polymer nanocomposites (NCs) generally have robustness, thermal stability, electrical conductivity and high chemical resistance and low weight. The nanoparticles (NPs) have the most applications as a reinforcing phases in NCs especially polymers. Adding metal and metal oxide NPs and some organic particles to the polymeric materials can improve the properties of polymers such as thermal stability, glass transition temperature, mechanical strength, thermal conductivity, heat resistance index, dispersibility, adhesion, and even adsorption capacity for bilirubin and etc.

Inorganic/polymer NCs are new classes of polymeric materials. These materials combine the properties of both components. It means that polymer component with excellent optical property, flexibility and toughness could improve the brittleness of inorganic particles and besides, inorganic particles could increase the strength and modulus of polymers [2]. Covering the surface of NPs with polymers is an effective method of surface modification that causes not only NPs to have good dispersion in organic media but also to be compatible with the polymer environment.

PMMA/NiO NCs were synthesized through in situ polymerization of MMA monomer in the presence of NiO NPs. The NiO NPs were prepared by Pechini method and its surface was modified with 3-mercaptopropyltrimethoxysilane.

✉ Esmaiel Soleimani
essoleimani@shahroodut.ac.ir; ssoleimani64@gmail.com

[1] Inorganic Chemistry Research Laboratory, Faculty of Chemistry, Shahrood University of Technology, Shahrood 3619995161, Iran

The thermal properties of PMMA/NiO NCs were investigated by TGA and compared to pure PMMA. From the results obtained, an improvement of the thermal stability of the NPs was observed; the thermal stability increases in the presence of the NiO NPs due to the restriction of mobility of the polymer chains [3].

Polystyrene is a thermoplastic polymer that has been widely used for its specific properties. The ease of transportation and the special characteristics of polystyrene have made this polymer one of the most widely used polymers in various industries such as the construction of car body and home appliances, building insulation and packaging industries [4].

Hybrid silica/polystyrene NCs were synthesized by mini-emulsion polymerization. With the objective to prepare core–shell hybrid NCs having narrow particle size distributions as well as a high degree of silica encapsulation, the effect of adding surface modifiers, the size of silica NPs, the ratio styrene/silica, the surfactant concentration, and the presence of ethanol in the reaction mixture were studied. Oleic acid was used to surface modification of the silica NPs that it forms the hydrogen bond with the hydroxyl groups on the surface of silica nanoparticles. Finally, a double bond of oleic acid will be able to polymerize with vinyl monomers. A synergistic effect was observed using oleic acid together with 3-(trimethoxysilyl)propyl methacrylate in the compatibilization step between the organic phase (monomer) and inorganic silica NPs [5].

Raspberry-like silica/polystyrene NCs, silica particle as core and polystyrene nodules as shell, were synthesized through mini-emulsion polymerization by using sodium dodecyl sulfate surfactant, hexadecane co-stabilizer in the presence of silica particles modified by methacryloxy(propyl)trimethoxysilane (MAPTMS) or *n*-octadecyltrimethoxysilane. In this unique process, it was found that the raspberry-like silica/polystyrene NCs could be obtained based on MAPTMS grafted silica NPs at high grafted density. The NCs could possess bigger shape stability due to coordinate effect of both the polymerizable group and hydrophobic interaction provided by MAPTMS molecules [6].

The SiO_2/polystyrene NCs were synthesized through mini-emulsion polymerization by using sodium lauryl sulfate surfactant, hexadecane co-stabilizer in the presence of silica NPs coated with methacryloxy(propyl)trimethoxysilane. Core–shell or other interesting morphology composite particles were obtained depending on the size of the silica particles and the surfactant concentration employed. By adjusting these parameters, it was possible to control the size and morphology of the composite particles [7].

Fe_3O_4/polystyrene NCs were prepared from oleic acid (OA) modified Fe_3O_4 NPs via mini-emulsion polymerization. It was concluded that the surface properties of OA modified magnetite nanoparticles have a great effect on preparation of the NCs. Fe_3O_4/polystyrene NCs with defined structure and different magnetite content can be readily prepared from monolayer OA modified Fe_3O_4 NPs. It was concluded that surface of the monolayer OA modified Fe_3O_4 NPs is hydrophobic, thus improving the dispersibility of the Fe_3O_4 NPs in styrene monomer and allowing preparation of the Fe_3O_4/polystyrene NCs with defined structure and controllable magnetite content [8].

The encapsulation of high amounts of magnetite into polystyrene particles can efficiently be achieved by a new three-step preparation route including two mini-emulsion processes. In the first step, a dispersion of oleic acid coated magnetite particles in acetone is obtained. In the second step, magnetite aggregates in water are produced in a mini-emulsion process by using sodium dodecyl sulfate (SDS) as surfactant. In the third step, the dispersion with the magnetite aggregates which are covered by an oleic acid/SDS bilayer were mixed with a monomer mini-emulsion and a second mini-emulsion process, and ad-mini-emulsification process, is used to obtain full encapsulation. After polymerization, polymer encapsulated magnetite aggregates were obtained. Characterization by TGA and TEM showed that up to 40% magnetite could be encapsulated resulting in particles with a high homogeneity of the magnetite content. Magnetometry measurements reveal that the included iron oxide aggregates still consist of separated superparamagnetic Fe_3O_4 particles [9].

A polystyrene/HgS NCs has been synthesized, and the effect of HgS filler on the physical properties of polystyrene/HgS NCs has been studied by using DSC and TGA. The glass transition temperature of NCs is higher than that of the pure polymer as a result of the low molecular mobility induced by the presence of filler nanoparticles. The TGA curve of NCs indicates a higher thermal stability for NCs as observed by the shift in onset temperature of degradation by about 12 °C relative to that of pure polystyrene [10].

The PSt/silica NCs were prepared by radical polymerization of silica NPs possessing vinyl groups and styrene with benzoyl peroxide. The results indicated that polystyrene had been successfully grafted onto vinyl silica NPs via covalent bond. Surface wetting properties of the PSt/silica NCs film were evaluated by measuring water contact angle and the sliding angle using a contact angle goniometer. The excellent superhydrophobic property enlarges potential applications of the superhydrophobic surfaces [11]. Sulfonated PSt microsphere were functionalized using ethylene diamine to introduce amine groups to the polymer chains. The amine functionalized polymers were used as a support for gold NPs. The PSt/Au NCs was found to be an efficient catalyst for the oxidation of alcohols in water [12].

The effect of silica NPs has been investigated on the adhesion of micron-sized PSt particles. When silica NPs were

added, an increase in the overall removal of PSt particles under a given centrifugal force was seen. The greatest effect was observed for the lowest silica NPs concentrations used [13]. A copper NPs colloid was synthesized by reduction of cupric sulfate with hydrazine hydrate in the presence of CTAB and PVP. A uniform Cu/PSt NCs was further synthesized via in situ emulsion polymerization. The morphologies, structures, as well as thermal stabilities of the Cu/PSt NCs were characterized. The TGA analysis indicates that the uniform Cu/PSt NCs has a better thermal stability than virgin polystyrene [14].

A novel $CaCO_3$/PSt NCs adsorbent was synthesized for efficient bilirubin removal from human plasma. A comparison with the PSt adsorbent, which was without the incorporation of nano-$CaCO_3$, revealed that $CaCO_3$/PSt NCs had superior bilirubin adsorption capacity and mechanical strength. The adsorption results indicated that $CaCO_3$/PSt NCs displayed better adsorption capacity for bilirubin than that of PSt. The mechanical strength of $CaCO_3$/PSt NCs was significantly greater than that of PSt. In addition, both $CaCO_3$/PSt NCs and PSt possessed good blood compatibility properties. Therefore, a conclusion could be drawn that $CaCO_3$/PSt NCs has a high potential as an efficient bilirubin adsorbent for blood purification in clinical practice. At the same time, the success of organic–inorganic NCs adsorbents might provide a new insight into the improvement of adsorbents in hemoperfusion [15].

The BN@PSt composites with high thermal conductivity were fabricated via suspension polymerization. Compared with traditional routes, the novel preparation process requires less BN fillers when improving the same thermal conductivity. Importantly, other polymers can also encapsulate BN through this strategy, which paves a new way for preparing thermally conductive polymer–matrix composites [16].

A series of PSt/silica NCs with different inorganic nanofiller content were prepared by evaporating of toluene solvent. The influence of the filler content on glass transition temperature of PSt/silica NCs was followed by DSC analysis. It was found that the polystyrene glass transition temperature was influenced by the hydrophobic silica content. A mathematical method to describe the glass transition temperature dependence on the PSt/silica ratio is proposed. According to the experimental results and calculations, the highest thermal stability of the NCs belongs to 18% silica content [17].

High thermal conductivity graphite nanoplatelet/ultra-high molecular weight polyethylene (GNPs/UHMWPE) NCs are fabricated via mechanical ball milling followed by a hot-pressing method. The thermal conductivity coefficient of the GNPs/UHMWPE NCs is greatly improved nine times higher than that of the original UHMWPE matrix. The significantly high improvement of the thermal conductivity is ascribed to the formation of multidimensional thermally conductive GNPs–GNPs networks, and the GNPs have a strong ability to form continuous thermally conductive networks. Furthermore, the thermal stabilities of the GNPs/UHMWPE NCs are increased with increasing addition of GNPs [18].

Hybrid fillers of micrometer boron nitride/nanometer boron nitride (*m*BN/*n*BN) were employed to fabricate the highly thermally conductive insulating *m*BN/*n*BN/polyphenylene sulfide ((*m*BN/*n*BN)/PPS) composites via mechanical ball-milling followed by hot-compression method. The thermally conductive coefficient, dielectric constant and dielectric loss tangent values and thermal stabilities were all enhanced with the increasing addition of *m*BN/*n*BN hybrid fillers. Appropriate addition of the *m*BN/*n*BN hybrid fillers played a role of heterogeneous nucleation for PPS matrix [19].

The proposed combining method of silane coupling agent of γ-aminopropyl triethoxy silane/aminopropyllsobutyl polyhedral oligomeric silsesquioxane was performed to functionalize the surface of hexagonal nanometer boron nitride fillers (*f*-*n*BN), aiming to fabricate the *f*-*n*BN/polyphenylene sulfide (*f*-*n*BN/PPS) NCs with excellent thermal conductivities, outstanding thermal stabilities and optimal dielectric properties. The usage of *f*-*n*BN fillers was benefit for improving the thermally conductive coefficient (λ) and decreasing dielectric constant (ε) values of the PPS NCs. The *f*-*n*BN/PPS NCs with 60 wt% *f*-BN fillers was an excellent dielectric NCs with high λ and ideal ε values and outstanding thermal stability, which holds potential for electronic packaging materials and ultra-high voltage electrical apparatus [20].

Both aminopropylisobutyl polyhedral oligomeric silsesquioxane (NH_2–POSS) and hydrazine monohydrate were utilized to functionalize graphene oxide (GO), and to obtain chemically modified graphene (CMG), which was then used for preparing thermally conductive CMG/polyimide (CMG/PI) NCs via a sequential in situ polymerization and electrospinning-hot press technology. NH_2–POSS molecules were grafted on the GO surface, and CMG was obtained by the reaction between NH_2–POSS and GO. The thermal conductivity coefficient (λ), glass transition temperature and heat resistance index of the prepared CMG/PI NCs were all increased with increasing the CMG loading. The λ value of the CMG/PI NCs with 5 wt% CMG was significantly improved four times higher than that of the pristine PI matrix [21].

In accordance with the above studies, and the continuation of our previous work [22], here, we are releasing a useful method to produce inorganic/polymer (NiO/PSt) NCs using oleic acid as modifier and then in situ mini-emulsion polymerization. The first NiO NPs was prepared from reaction of $Ni(NO_3)_2{\cdot}6H_2O$ with sodium hypochlorite in the present of CTAB in alkaline solution, and then its oxidation by

ethanol. The surface of as-synthesized NiO NPs was modified by oleic acid in order to obtain better dispersibility and proper compatibility in organic media. At last PSt/NiO NCs were synthesized via in situ mini-emulsion polymerization. The modified NiO NPs were dispersed in water phase in an ultrasound bath to prevent the aggregation of NPs, and then mini-emulsion polymerization was performed in the presence of modified NiO NPs. From this study, it was found that one of key requirements in the synthesis of inorganic/polymer NCs was the enhanced interfacial compatibility between inorganic and polymer, which was achieved by treating the surface of inorganics with an organic modifier such as oleic acid. These compounds were characterized by FT-IR spectroscopy, X-ray diffraction (XRD), scanning electronic microscopy (SEM), energy dispersive X-ray spectroscopy (EDX), X-ray photoelectron spectra (XPS) and vibrating sample magnetometer (VSM). Finally, thermal stability of PSt/NiO NCs was studied by techniques of TGA and DSC analysis.

2 Experimental

2.1 Materials

In this work the chemicals such as oleic acid, $Ni(NO_3)_2{\cdot}6H_2O$, NaOH, methanol, ethanol (96%), sodium dodecyl sulfate (SDS, 99%), styrene (99.9%), Cetyl trimethylammonium bromide (CTAB, 99%), ammonium peroxodisulfate (APS, 99.5%), sodium hypochlorite, $NaHCO_3$ (98%) and hexadecane (99%) were used as purchased from the chemical company (Merck) without any purification.

2.2 Characterization

X-ray diffraction patterns of powder samples were recorded by XRD system BRUKER-D8. The surface morphology and shape of the nanoparticles were examined using field emission scanning electron microscopy (FE-SEM; Hitachi SU6600, Japan) and The chemical composition of the NPs was examined using electron dispersion X-ray spectroscopy (EDX; EMAX, Horiba 8121-H, Japan). Infrared spectroscopy (FT-IR) experiments were recorded on a Perkin Elmer 1760-X spectrometer. Thermo-gravimetric analysis (TGA) was carried out on a HT-503 thermo-analyzer (Netzsch, Germany), under argon atmosphere, heating rate 10 °C min^{-1}. X-ray photoelectron spectroscopy (XPS) of the as-prepared NiO nanopowder was measured on an ESCA-3000 electron spectrometer with monochromatized Mg Kα X-ray as the excitation source. The magnetic characterization of the nanomaterials was carried out in a vibrating sample magnetometer (VSM; BHV-55, Riken, Japan) at room temperature.

2.3 The procedure of materials preparation

2.3.1 Preparation of NiO NPs

The NiO NPs precursors were synthesized by the precipitation method and then calcination of sediment. Firstly, 1.25 g of CTAB dissolved in 20 mL of water under ultrasonic bath at room temperature for 20 min. It was added to 1.45 g of nickel(II) nitrate (5 mmol) dissolved in 5 mL of water under ultrasonic bath. The mixture was placed under a magnetic stirrer at 1000 rpm for 15 min. Then 0.4 g of sodium hydroxide (10 mmol) was dissolved in 3.75 mL of sodium hypochlorite solution and it added to the above mixture with together magnetic stirrer which formed a black precipitate for 20 min. Then, 10 mL of ethanol was added to mixture containing precipitate black (nickel peroxide) under a magnetic stirrer at 1000 rpm for 2 h until it was formed an olive-green deposition of NiO. The resulting precipitates was washed several times with distilled water (10 mL) and ethanol (5 mL) respectively and dried in an oven at 90 °C for 6 h. Finally, the precipitates were calcined in a furnace at 300 °C for 2 h to create NPs with suitable crystalline structure.

2.3.2 Surface modification of NiO NPs

0.25 g of NiO NPs were added to 5 mL oleic acid solution (3% V in ethanol) and mixed in ultrasonic bath at room temperature for 10 min. The suspension was heated at 65 °C on a hot plate magnetic stirrer with 750 rpm for 4 h. The modified NPs were separated by centrifuges from the mixture and dispersed in 10 mL of ethanol under ultrasonic bath to remove the oleic acid residues. The precipitates were filtered and washed several times with ethanol and water, and dried in an oven at 40 °C for 24 h.

2.3.3 Preparation of PSt

First, 0.1 g hexadecane (0.13 mL) was added to 2 g of styrene (2.2 mL) and was placed in an ultrasonic bath at room temperature for 10 min. It was added to a solution of 0.08 g of SDS and 0.028 g of $NaHCO_3$ dissolved in 30 mL of water under ultrasonic bath. The mixture was placed under a magnetic stirrer at 1000 rpm for 15 min. The mixture was then placed in an ice-water bath under a 200 V ultrasonic homogenizer (7 s pulse, 3 s silencing) for 30 min. The completely uniform solution was transferred to a three-neck balloon equipped with nitrogen gas and heated at 75 °C in an oil bath. 0.03 g of potassium persulfate (KPS) in 3 mL of water was added slowly to solution and the polymerization process was carried out in a magnetic stirrer with 300 rpm at 75 °C for 8 h. The resulting polystyrene was separated from the mixture and dried at room temperature. Polystyrene was

dispersed in 100 mL of water under magnetic stirring for 30 min and then dispersed in 20 mL of ethanol under magnetic stirring for 30 min to remove impurities such as SDS, KPS, hexadecane and styrene. The resulting precipitates was washed several times with water (10 mL) and ethanol (5 mL) respectively and dried at room temperature for 6 h.

2.3.4 Preparation of PSt/NiO NCs

First, 0.1 g hexadecane (0.13 mL) was added to 2.0 g of styrene (2.2 mL) and placed in an ultrasonic bath at room temperature for 10 min. Second, 0.1 g of modified NiO NPs (5% wt relative to the monomer) was dispersed in hexadecane and styrene solution and then was exposed under ultrasound for 15 min. It was added to a solution of 0.08 g of SDS and 0.028 g of $NaHCO_3$ dissolved in 30 mL of water under ultrasonic bath. The emulsion was placed under a magnetic stirrer at 1000 rpm for 15 min. The mixture was then placed in an ice-water bath under a 200 V ultrasonic homogenizer (7 s pulse, 3 s silencing) for 30 min. The completely uniform mini-emulsion was transferred to a three-pronged balloon equipped with nitrogen gas. The mini-emulsion was deoxygenating by bubbling nitrogen gas through the solution for 20 min and heated at 75 °C in an oil bath. 0.03 g of potassium persulfate (KPS) in 3 mL of water was added slowly to solution under nitrogen atmosphere and the polymerization process was carried out in a magnetic stirrer with 300 rpm at 75 °C for 8 h. The resulting PSt/NiO NCs was separated from the mixture and dried at room temperature. The polymeric NCs was dispersed in 100 mL of water under magnetic stirring for 30 min and then dispersed in 20 mL of ethanol under magnetic stirring for 30 min to remove impurities such as SDS, KPS, hexadecane and styrene. The resulting precipitates was washed several times with water (10 mL) and ethanol (5 mL) respectively and dried at room temperature for 6 h.

2.4 Measurement of lipophilic degree

One way of measuring lipophilic degree (LD) of the surface of NPs is to disperse a certain amount of NPs in water, and then to carry out titration with an organic solvent such as methanol [22–24]. When NiO NPs are added to water, sedimentation takes place promptly, whereas the NiO NPs modified by oleic acid will float and disperse in water. By adding drop wise of methanol from a burette to a dispersed solution of modified NiO NPs (0.1 g in 10 mL water), the modified NPs gradually precipitate. Knowing the volume of methanol used, LD of modified NPs can be calculated using the following Eq. (1):

$$\mathrm{LD} = \frac{\mathrm{V}}{\mathrm{V}+10} \times 100 \tag{1}$$

In this equation, V is the volume of methanol used in mL, and 10 is the initial volume of water. The LD of modified NiO NPs caused by varying amount of oleic acid was measured by the above method. Measurements of the LD were used as a guide to evaluate the procedure used for surface modification.

2.5 Effective factors on lipophilic degree

The factors that effect on LD are: Amount of fatty acids, reaction temperature and mixing time. In this study, factors were varied one at a time while the rest of the factors were kept constant.

2.5.1 Effect of amount of modifier

Different amount of oleic acid (0.05, 0.15, 0.25, 0.35, and 0.45 mL) were dissolved in 5 mL ethanol. Then 0.25 g of NiO NPs was added to the above solution, and was refluxed at 65 °C for 4 h. The precipitates were separated, washed three times with ethanol and dried in an oven at 50 °C for 24 h. The modified NiO NPs were separated by centrifuges from the mixture and dispersed in 10 mL of ethanol under ultrasonic bath to remove the oleic acid residues. The precipitates were filtered and washed several times with ethanol and water, and dried in an oven at 40 °C for 24 h. The following experiment was conducted to determine LD of modified NiO NPs: first 0.10 g of modified NiO NPs is added to 10 mL water. Then methanol is added dropwise through a burette to these dispersed NPs until no more sediment is formed. The volume of methanol is used to calculate LD of the surface of modified NPs, according to Eq. (1).

2.5.2 Effect of mixing time on the modification

0.25 g NiO NPs was added to a solution of 0.50 mL oleic acid in 10 mL ethanol. The mixture was stirred at 65 °C for different length of time (1, 2, 3, 4, 5, and 6 h). The precipitates were separated, washed three times with ethanol, and dried in an oven at 40 °C for 24 h. The method used for determining LD of modified NiO NPs is similar to afore-mentioned method, according to Eq. (1).

2.5.3 Effect of temperature on the modification

0.25 g modified NiO NPs was added to a solution of 0.50 mL oleic acid in 10 mL ethanol. The mixture was stirred for 4 h at different temperatures (25, 35, 50, 65, and 75 °C). The precipitates were separated, washed three times with ethanol and dried in an oven at 400 °C for 24 h. The method used for determining lipophilic degree of modified NiO NPs is similar to afore-mentioned method, according to Eq. (1).

3 Results and discussion

It was necessary to use NiO NPs as a precursor for the synthesis of PSt/NiO NCs. Therefore, a new method has been proposed for the preparation of high purity NiO NPs from the combination of well-known methods and our research experience [22, 25]. The NiO NPs have been prepared by a simple and efficient chemical precipitation method with the aid of a surfactant. NiO_2 was first prepared by oxidation of $Ni(NO_3)_2{\cdot}6H_2O$ with hypochlorite solution. The as-prepared NiO_2 was then easily converted to NiO NPs merely by treating it with ethanol at room temperature. In our procedure there is no need for controlling the pH of the solution, as it usually required in most of the chemical precipitation methods. More importantly, calcinations at high temperature, which is used in other similar routes, have been eliminated in the present method. Therefore, this method can be introduced as an inexpensive, fast and reproducible process for the large-scale synthesis of NiO nanocrystals. The use of cationic surfactant CTAB which produced smaller sized NiO NPs is recommended for this purpose. The reaction equations are as follows:

$$Ni(NO_3)_2 \cdot 6H_2O + NaOH + NaOCl \rightarrow NiO_2 \downarrow + 2NaNO_3 + HCl + 6H_2O \quad (2)$$

$$NiO_2 + CH_3CH_2OH \rightarrow NiO + CH_3CHO + H_2O \quad (3)$$

The preparation method of NiO NPs has a unique advantage. Because it does not use expensive materials and precursors are easily available. The NiO NPs is an inorganic material, while styrene is an organic matter. So for incorporation of inorganic NiO into organic polymer, it is necessary that the NiO NPs to be modified by oleic acid. Oleic acid has a carboxyl group and a double bond. These might facilitate polymerization process of styrene on the surface of NiO NPs. First carboxylic group of oleic acid react with the hydroxyl group on surface of NiO NPs. Then unsaturated double bond (C=C) is added to styrene monomer through the radical polymerization and using potassium peroxodisulfate (KPS) as radical initiator to produce PSt/NiO NCs.

In order to confirm as-synthesized NiO NPs, its modification by oleic acid, and PSt/NiO NCs were studied by the usual methods of identification and morphology consideration.

3.1 X-ray diffraction patterns

X-ray diffraction patterns of NiO NPs and PSt/NiO NCs were recorded, and the results are shown in Fig. 1. The five characteristic angles viz 2θ equal to 37.2, 43.3, 62.8, 75.2, and 79.4°, which well correspond to the standard card

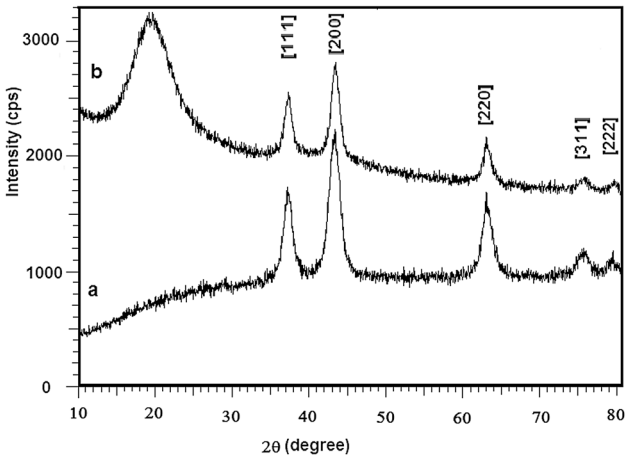

Fig. 1 XRD diffraction patterns of (**a**) bare NiO NPs and (**b**) PSt/NiO NCs

JCPDS-04-0835, which confirms that the crystal structure of NiO NPs is face centered cubic with cell constant a = 4.171 Å [26, 27]. These peaks correspond to the diffraction lines of crystal plates of [111], [200], [220], [311] and [222] of cubic phase of NiO respectively. Since no peaks of impurity were observed, means that the high purity NiO was obtained. Figure 1a, b show that the characteristics of peaks of NiO has not changed even after its accession to the polymer, and are the same as those of bare NiO NPs with face centered cubic crystal structure. The sharp and intense peaks indicate that sample is highly crystalline. The average crystallite sizes of bare NiO NPs and PSt/NiO NCs that are calculated from XRD diffraction patterns according to Debye-Sherrer formula $D = K\lambda/\beta\cos\theta$ are 17.0 and 21.0 nm respectively. In this equation constant: K = 0.89, wave length of incident light λ = 1.54 Å and β is the half width of the most intensive peak.

Embedded polystyrene to NiO NPs reduced crystallinity of NPs, so that the height and intensity peak of NCs is reduced (Fig. 1b). This indicates that polystyrene is linked to crystal plates of NiO NPs in all directions [28]. In this XRD diffraction pattern (Fig. 1b) was observed an additional broad peak at 19° which can be attributed to the presence of polystyrene in NiO NCs [29].

3.2 FT-IR spectra

In order to study the bonds formed, FT-IR spectra of NiO NPs were recorded before and after surface modification by oleic acid. These spectra are shown in Fig. 2. The broad band observed in the FT-IR spectrum of NiO NPs (Fig. 2a) at 3411 cm^{-1} corresponded to O–H stretching vibration of

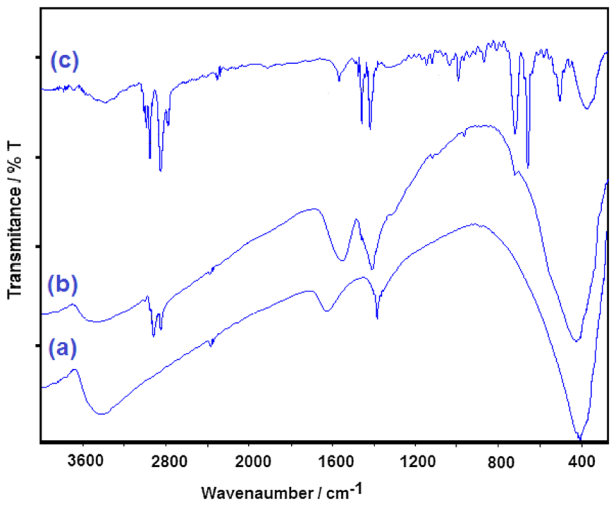

Fig. 2 FT-IR spectra of (**a**) bare NiO NPs; (**b**) modified NiO NPs by oleic acid; (**c**) PSt/NiO NCs

water molecules on the surface of NPs [30, 31]. Bending vibration of this bond has been observed at 1624 cm^{-1} [31, 32]. The band at 1384 cm^{-1} is due to the presence of carbonate anion and the strong absorption band at 411 cm^{-1} is related to stretching vibration of Ni–O bond [33, 34]. The bands at 3411 and 1384 cm^{-1} in Fig. 2a are due to the fact that the calcined powders tend to physically absorb water and carbonate ions, respectively.

Hydroxyl groups should be present at its surface to modify the surface of the NPs by oleic acid. The FT-IR spectrum clearly shows the presence of hydroxyl groups on the surface of NiO NPs. The point to be noted is the absence of a sharp peak at 3640 cm^{-1}, since the presence of this band could prove the structure of $Ni(OH)_2$ NPs. Therefore, it is necessary to control the calcination temperature for the preparation of NiO NPs with superficial hydroxyl groups [34, 35]. Figure 2b are shown FT-IR spectrum of NiO NPs modified by oleic acid. In addition to band as for Ni-O stretching vibration at 422 cm^{-1}, bands were observed at 3468, 2920, 2851, 1551, and 1406 cm^{-1}.

The band at 3468 cm^{-1} is due to the stretching vibration of hydroxyl groups on the surface of NPs modified with oleic acid [28, 32]. It dropped in intensity compared to the previous peak, which represents grafting oleic acid on the surface of modified NiO NPs. Two absorption bands at 2920 and 2851 cm^{-1} in the FT-IR spectra of NiO NPs modified by oleic acid are due to vibration frequencies of methyl and methylene group of oleic acid covering the surface of NPs [32, 36, 37]. Two other bonds viz bands at 1551 and 1406 cm^{-1} can be allocated to symmetric and asymmetric vibration of carbonyl group (C=O) of carboxylate moiety of oleic acid which cover the surface of NiO NPs [38, 39]. The difference between the two bands of 145 cm^{-1}, indicates the bidentate character of oleate ($–COO^–$) to surface of modified NiO NPs [40]. Also, the band at 1624 cm^{-1} belong to bending frequency of OH was not observed in modified NPs which indicate the surface modification of NiO NPs by oleic acid.

The observation of these four absorption bands confirms that the surface of NiO NPs was modified by oleic acid. On the other hand, stretching frequencies of carbonyl group in the range of 1700–1725 cm^{-1} related to oleic acid free is not observed [38]. This behavior suggests that a single molecular layer is composed of oleic acid on the surface of NiO NPs [38, 41].

Figure 2c are shown FT-IR spectrum of PSt/NiO NCs. Two bands observed in the regions of 697 and 755 cm^{-1} related to the bending vibrational modes of C-H outside the plate of the benzene ring, three bands at 1451, 1492, and 1601 cm^{-1} attributed to the C–C stretching vibrational modes of the benzene ring, two bands at 2849 and 2929 cm^{-1} correspond to the vibrational frequencies of aliphatic C–H bond, and a band at 3026 cm^{-1} belong to stretching frequencies of aromatic C–H bond [42]. These results indicate that polystyrene is grafted to the surface modified NiO NPs. Another beak was observed at 444 cm^{-1} which is related to the stretching vibration of Ni–O bond in NiO NPs. The vibrational displacement at 422 cm^{-1} in modified NiO NPs to 444 cm^{-1} in PSt/NiO NCs indicates a strong interaction between polystyrene and modified NiO NPs [43]. This interaction is shown in Scheme 1.

3.3 SEM images and EDX analysis

The NPs have a tendency to aggregate because their surface energy is high. Therefore, surface modification is expected to decrease aggregation and improve dispersion [44–46]. Thus, for studying dispersion, SEM images of NiO NPs, NiO NPs modified by oleic acid and PSt/NiO NCs have been recorded which is shown in Fig. 3.

As can be seen in Fig. 3a, the surface morphology of bare NiO NPs are stuck together and aggregated which is due to large surface area to volume ratio and high energy of the surface of NPs. Whereas in Fig. 3b NiO NPs modified by oleic acid composed of non-uniform particles and irregular layer put together and dispersed. This improvement dispersion of NPs certainly confirms the surface modification of NPs by oleic acid. The average particle size for both of them is approximately the same and equal to 16 nm in SEM images. As can be seen in Fig. 3c, the PSt/NiO NCs are completely spherical particles and like dandelion flower. The NCs were well distributed in the matrix and produce excellent dispersion. The size of these particles is about 45 nm. The particle size is larger because of their distribution in the polymeric tissue. These values are in good agreement with the average particle size calculated from the XRD patterns.

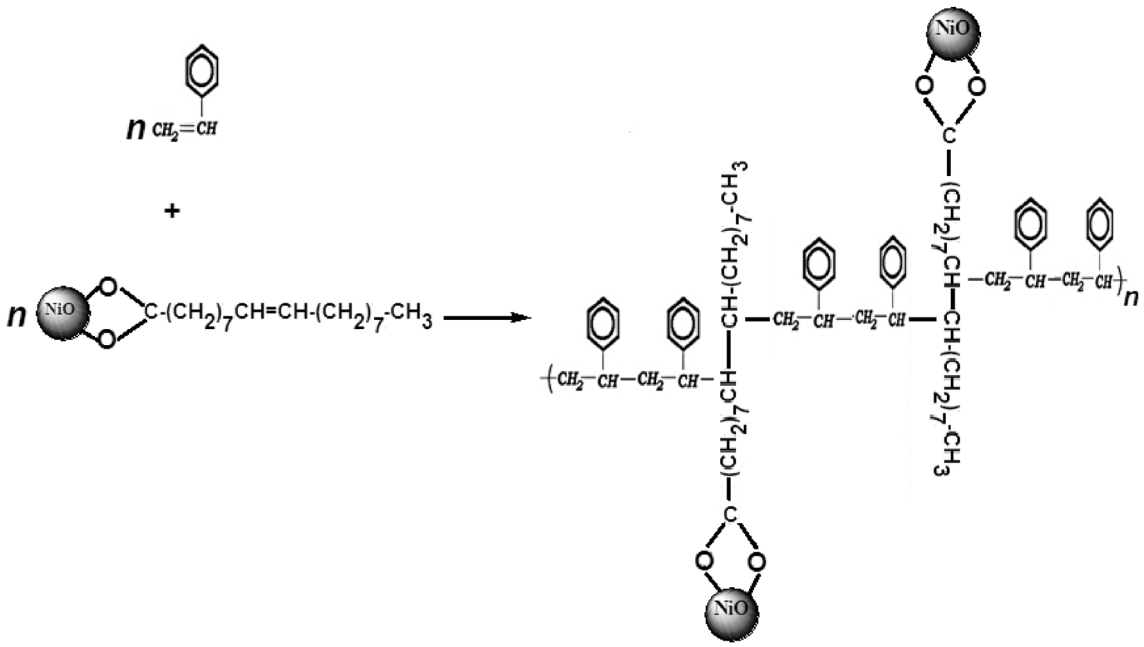

Scheme 1 Reaction equation for strong interaction between polystyrene and modified NiO NPs

A comparison of the SEM images of NiO NPs, NiO NPs modified with oleic acid, and NiO-PMMA PNCs can be concluded that modifying the surface of NiO NPs by oleic acid and incorporation of the NPs to PMMA changes the morphology of particles. In addition, the particles are distributed better and more uniformly in the PNCs, so that was created a monodispersion.

The EDX spectra of NiO NPs and its modified form by oleic acid and PSt/NiO NCs are shown in Fig. 4. The EDX spectrum given in Fig. 4a shows the presence of Ni and O as the only elementary components of NiO NPs. The presence of carbon, nickel and oxygen in NiO NPs is the proof for surface modification of oleic acid on NiO NPs (Fig. 4b), which was absent in bare NiO NPs. The percentage of carbon observed in EDX spectrum of PSt/NiO NCs is high (Fig. 4c), which is due to the presence of large amounts of polymer material, which contains carbon and hydrogen elements.

3.4 XPS spectra

Further evidence for the purity and composition of the products was obtained by X-ray photoelectron spectra (XPS). Figure 5 shows XPS spectra taken from the Ni and O regions of NiO NPs and PSt/NiO NCs. The data show that NiO is present in both samples. The binding energies of $Ni2p_{1/2}$, $Ni2p_{3/2}$ and O1s, provided a fairly complete picture of the sample powder. Two peaks observed at about 853.7 and 872.8 eV (Fig. 5a, b) are corresponded to $Ni2p_{3/2}$ and $Ni2p_{1/2}$ of Ni^{2+} in NiO NPs respectively [3]. The gap between the $Ni2p_{1/2}$ and $Ni2p_{3/2}$ level is 18.5 eV, consistent with the split orbit for Ni^{2+} ion no metallic Ni. The spectra for the NiO NPs embedded in polystyrene shown in Fig. 5b shows similar features than those observed in bare NiO NPs. The lower intensity is attributed to the surface functionalization of the NiO NPs. The functionalizing film in the NiO NPs lowers the number of photoelectron reaching the detector, resulting in lower intensity [3]. The peak at 530.8 eV in the O1s region (Fig. 5c, d) is attributed to the (O^{2-}) in the NiO NPs and PSt/NiO NCs [47].

3.5 Effective factors on lipophilic degree

The lipophilic degree (LD) of modified NiO NPs was used in order to provide appropriate conditions for the surface modification of NiO NPs. In achieving this aim, various factors such as reaction time, amount of modifiers, and reaction temperature were considered. The surface lipophilic of NPs was determined through a certain amount of NPs dispersed in water and then titrated with organic solvent [22–24, 40].

3.5.1 The amount of surface modifier

Different amount of oleic acid (1.0, 2.0, 5.0, 7.0, and 9.0% V) as surface modifier were applied on NiO NPs, and LD of the modified NiO NPs was measured according to the Eq. (1). The results obtained are shown in Table 1 as the variation of lipophilicity versus amount of oleic acid as modifier.

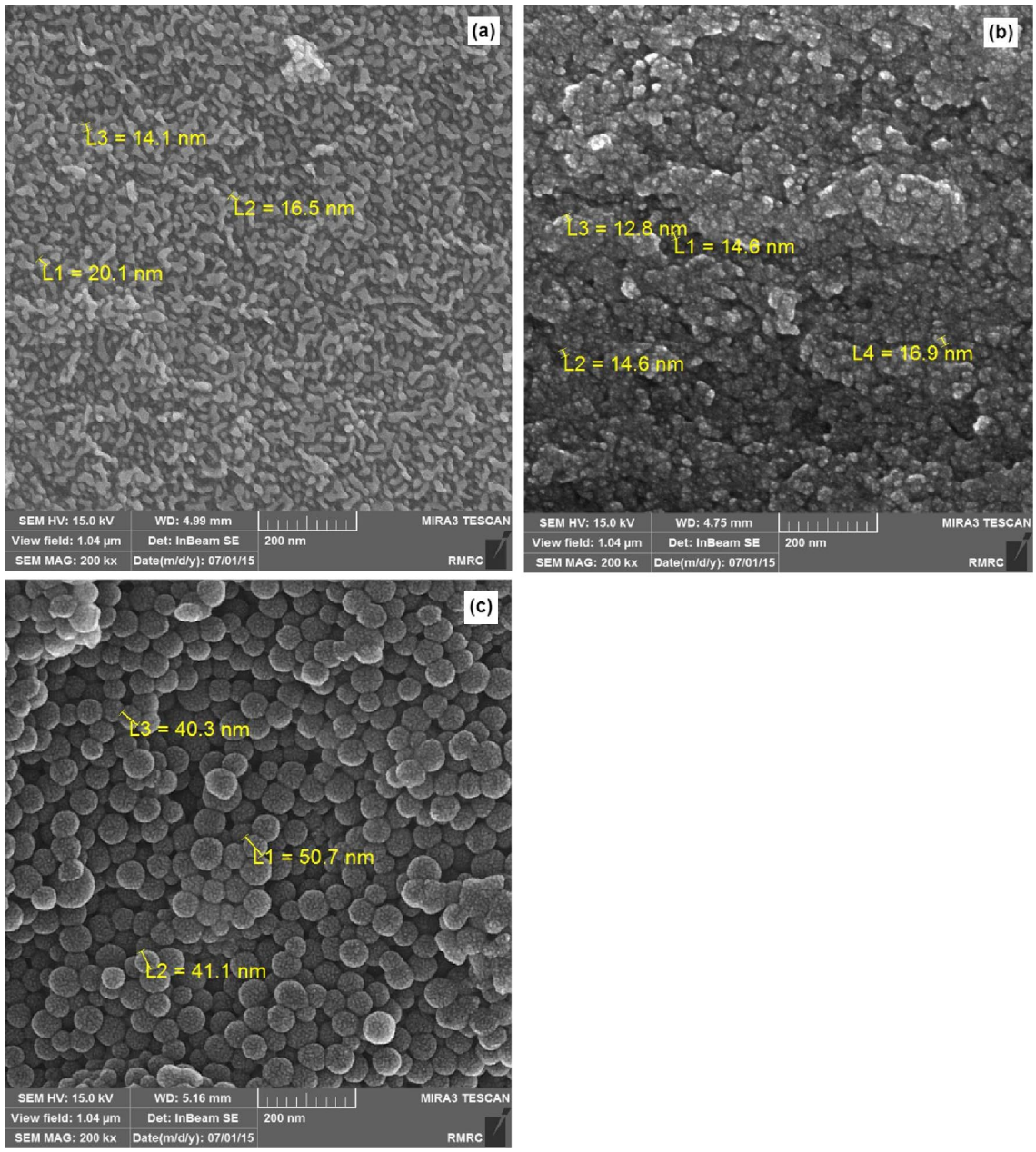

Fig. 3 SEM images of (**a**) NiO NPs; (**b**) NiO NPs modified by oleic acid; (**c**) PSt/NiO NCs

It can be seen from data that lipophilicity increases with the increase of amount of modifier up to 5% V. But lipophilicity is decreased if amount of the modifier increases to more than this value. The reason may be due to enlarging of the long chain hydrocarbon of the modifier which can stop the carboxylic group (–COOH) of oleic acid to react with the hydroxyl group on the surface of NiO NPs [48]. Therefore, from the present data, the optimum value of surface modifier is 5% V.

3.5.2 Effect of reaction time

It may be expected that when NiO NPs are mixed with oleic acid, the surface lipophilicity to vary to some extent. Therefore it was planned to put some of the NiO NPs in a solution of oleic acid in ethanol, and stir the solution for a certain time (1, 2, 3, 4, 5, and 6 h), and then to measure the LD of the modified NiO NPs. The measurements were carried out, and the results are shown in Table 2 as a variation of

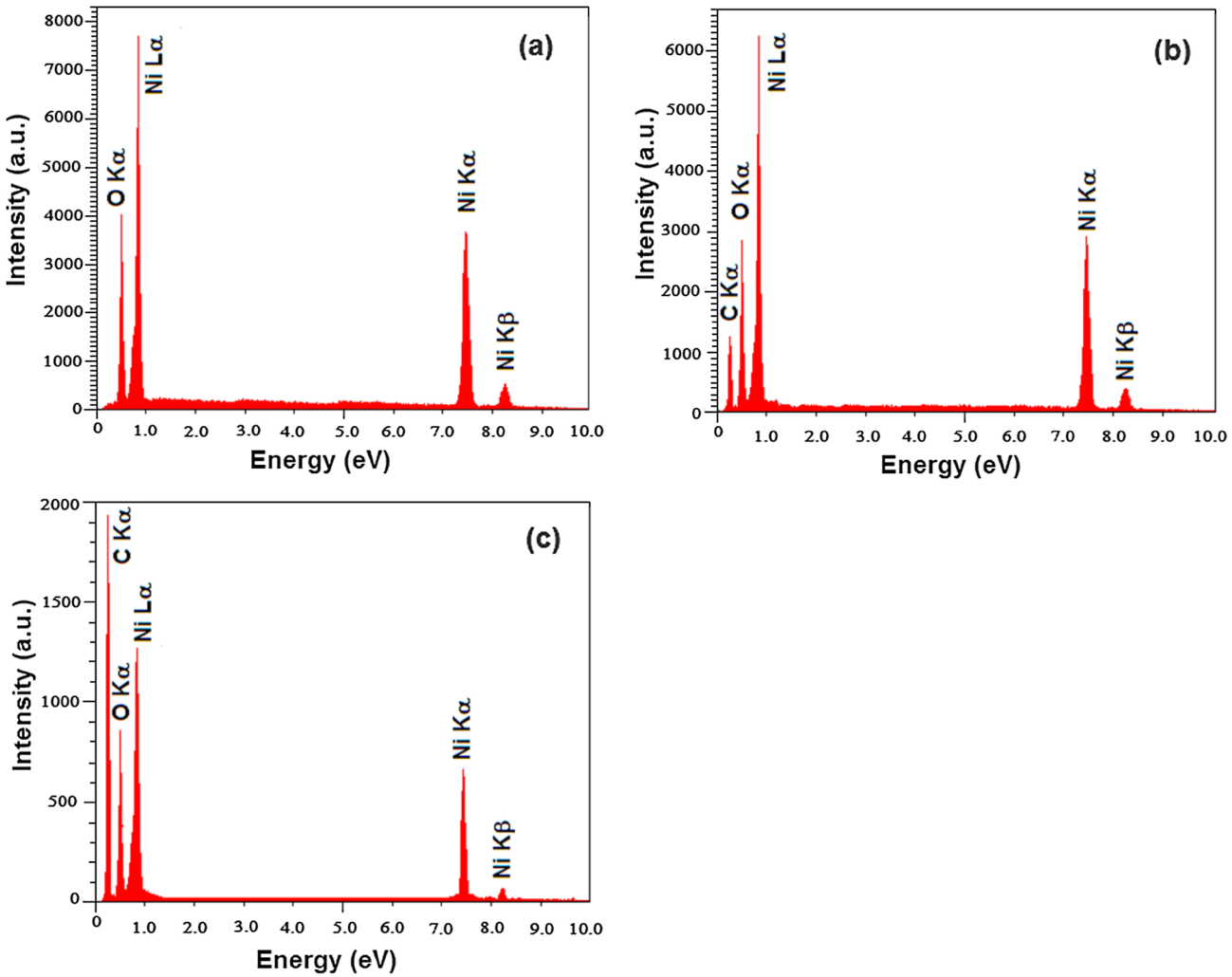

Fig. 4 EDX spectra of (**a**) NiO NPs; (**b**) NiO NPs modified by oleic acid; (**c**) PSt/NiO NCs

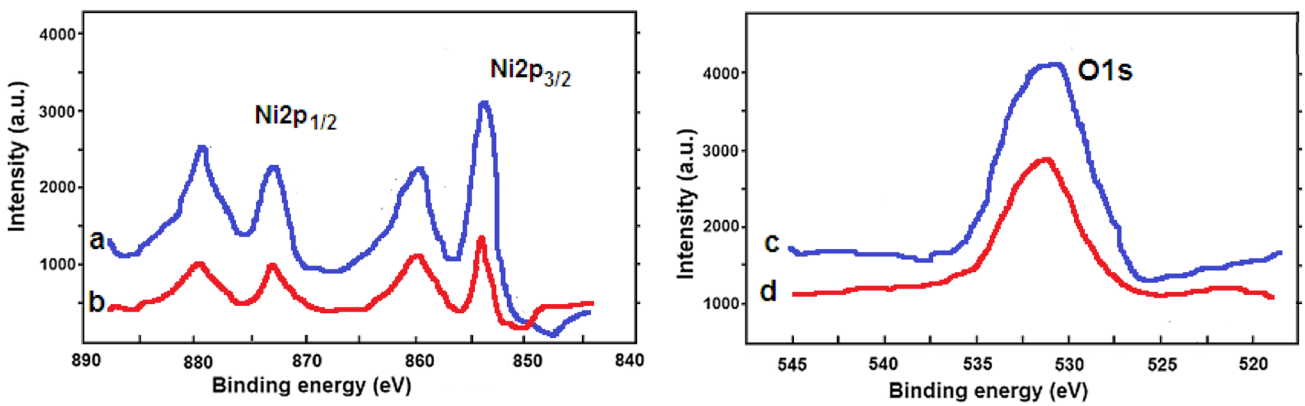

Fig. 5 XPS spectra of Ni region for NiO NPs (**a**) and PSt/NiO NCs (**b**) and oxygen region for NiO NPs (**c**) and PSt/NiO NCs (**d**)

Table 1 LD of modified NiO NPs (%) in different amount of modifier

Amount of oleic acid (% V)	1.0	3.0	5.0	7.0	9.0
LD of modified NiO NPs (%)	4.76	13.79	20.63	15.25	9.91

Reaction conditions: amount of NiO NPs 0.25 g, ethanol as solvent 10 mL, temperature 65 °C and reaction time 4 h

lipophilicity versus length of reaction time. It can be seen from data that the lipophilicity increases with increase of reaction time up to 4 h, but then it decreases if stirring is continued. Thus, the optimum lipophilicity is reached for 4 h of reaction time.

3.5.3 Effect of temperature on surface modification

The certain amounts of NiO NPs were stirred in a solution of oleic acid in ethanol at different temperature (25, 35, 50, 65, and 75 °C) for 3 h. Then LD of modified NiO NPs was measured. The results were then considered as variation of lipophilicity versus different temperature in Table 3. Similarly, in this case high lipophilicity is also a sign of good modification of the surface of NiO NPs. The highest lipophilicity is observed for oleic acid modifier of NPs at 65 °C. On the other hand, the increase in temperature has decreased the surface lipophilicity. Therefore from these results it can be concluded that the optimum temperature for the surface modification on NiO NPs is at 65 °C.

In this study, the NiO NPs should be modified before being joined to the polymer. The NiO NPs was modified with oleic acid. Other NPs were also modified by oleic acid [22, 23, 25, 40, 49, 50]. The optimum conditions for the amount of modifier and the reaction temperature and the reaction time are 5% V, 65 °C and 4 h, respectively.

3.6 TGA/DTA analysis

In order to evaluate thermal stability of PSt/NiO NCs, thermal analysis polystyrene (PSt) and PSt/NiO NCs were recorded. Thermal gravimetric analysis of PSt and PSt/NiO NCs was carried out under argon atmosphere, temperature range 25–600 °C and scan rate 10 °C/min.

Thermal Analysis curve for polystyrene is shown in Fig. 6a. TGA curves of polystyrene have shown that weight loss occurred in a two-step process, which is related to the destruction of polymer chains. Starting temperature of

Table 3 LD of modified NiO NPs (%) in different reaction temperature

Reaction temperature (°C)	25	35	50	65	75
LD of NPs modified by oleic (%)	7.41	11.89	15.91	22.21	14.16

Reaction conditions: NiO NPs 0.25 g, ethanol as solvent 10 mL, reaction time 4 h, and amount of oleic acid 0.50 mL

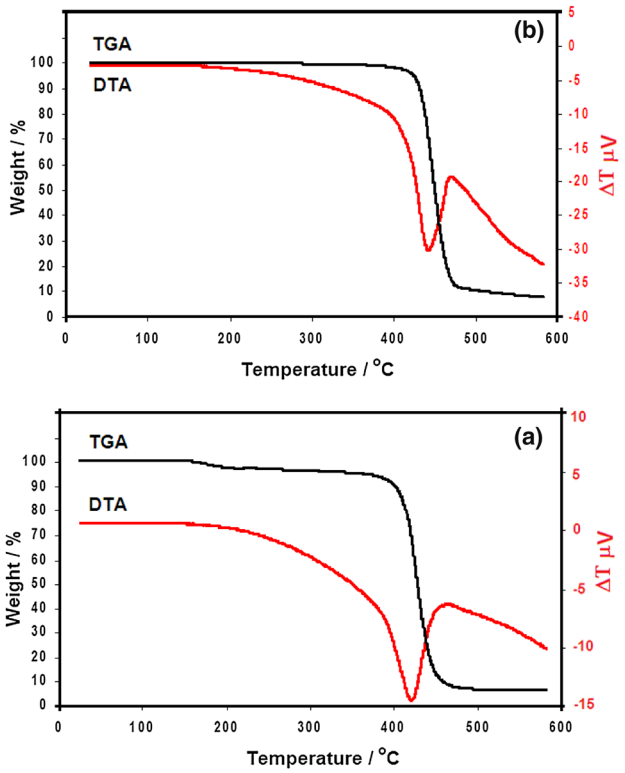

Fig. 6 The thermal analysis curves of: (**a**) polystyrene; (**b**) PSt/NiO NCs

weight loss occurred at 180 °C; that means the polymer can remain stable up to this temperature; and higher temperature is thermal instability. The first step of weight loss happened in the range of 180–200 °C with a weigh loss of 4% which is attributed to the degradation of polymeric chains with lower molecular weight. The second stage of weight loss occurred in the temperature range of 384–500 °C. The second stage of weight loss with amount of 96% is associated with an endothermic process at 421 °C in the DTA curve that is related

Table 2 LD of modified NiO NPs (%) in different reaction time

Reaction time (h)	1	2	3	4	5	6
LD of NPs modified by oleic (%)	11.5	14.5	16.67	21.36	15.97	15.75

Reaction conditions: NiO NPs 0.25 g, ethanol as solvent 10 mL, temperature 65 °C and amount of oleic acid 0.50 mL

to the destruction of polymer chains with higher molecular weight [51]. At temperatures above 500 °C nothing remains of polymer that means the entire polymer is destroyed.

Thermal analysis curves for PSt/NiO NCs is shown in Fig. 6b. A similar behavior of polystyrene is observed in thermal analysis for PSt/NiO NCs with a difference in that the starting temperature of weight loss occurred at 330 °C instead. So it can be concluded that the stable temperature has risen to 330 °C due to NiO NPs anchoring to the polymer. The stable temperature of polymer will increase about 150 °C due to incorporation of NPs into the polymer. Unlike polymer (PSt), the process of weight loss occurs in one step for PSt/NiO NCs in the temperature range 330–500 °C with a weigh loss of 95% which is associated with an endothermic process at 442 °C in the DTA curve. This corresponds to the destruction of the polymer (PSt) on the surface of NiO NPs [8, 51]. The remaining 5% of weight in the TGA curve corresponds to the NiO NPs after complete combustion of polymeric NCs. Thermal data can be concluded that the polymeric NCs contain 5 wt% NiO NPs. For this reason, the thermal stability of the polymeric NCs increased about 150 °C.

3.7 DSC analysis

In order to evaluate the effect of incorporation of NiO NPs on glass transition temperature of polymeric NCs, DSC thermo-graphic for polystyrene and PSt/NiO NCs were recorded and shown in Fig. 7.

The glass transition temperature was observed at 68 °C for polystyrene and 100 °C for PSt/NiO NCs. The glass transition temperature (Tg) is a standard for the degree of rotational freedom. The plastic property of a thermoplastic polymer is further enhanced if the glass transition temperature is lower. Improvement in the temperature of glass transition of polystyrene is difficult due to the rigidity of phenyl rings. This improvement occurs when polymer components are well absorbed onto the surface of the nanoparticles. It decreases the free space to move polymer macromolecules. Thus, a behavioral improvement in the glass transition temperature suggests a strong chemical bond between nanoparticles and polymer chains. The results of the DSC analysis show that the glass transition temperature increased by 32 °C with the addition of 5 wt% of NiO NPs in the polymer matrix.

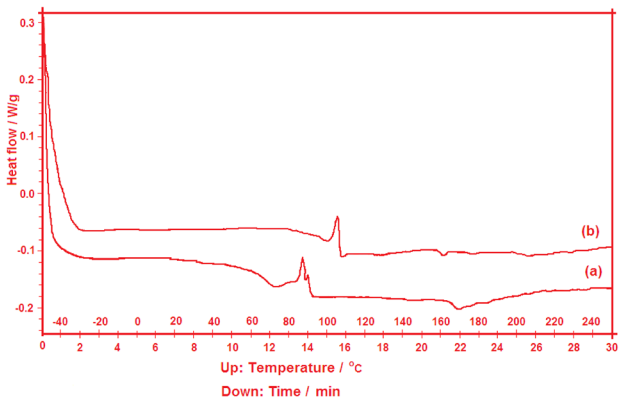

Fig. 7 DSC thermo-graphic for polymers: (**a**) polystyrene; (**b**) PSt/NiO NCs polymeric

Polymer crystallization process is observed at two temperatures of 87 and 91 °C (exothermic), and its melting temperature is 170 °C (endothermic). For this procedure, the crystallization and melting temperature of PSt/NiO NCs were observed at 106 and 160 °C respectively. Therefore the polymer performance increases where polymer flexibility has an important role. This change shows that the mobility of polymeric chains decreased in the presence of NiO NPs and subsequently has become more ordered. Energy crystallinity of the polymeric chains increases with increasing regularity and finally causes the glass transition temperature to increase.

Increasing the thermal stability of plastics causes their resistance to decomposition, disintegration by heat, mechanical cutting or oxidation reactions. On the other hand, an increase in the glass transition temperature in this group of polymers causes the paste to form at higher temperatures, which will reduce their permeability. It is therefore used a variety of fillers to achieve higher thermal stability and an improvement in the glass transition temperature of plastics.

In this study, NiO NPs were considered as a reinforcement of the polystyrene matrix because they have excellent thermal properties. The thermal analysis results (TGA/DTA and DSC) showed that the thermal resistance and glass transition temperature of polystyrene was improved for 45 and 29 °C respectively. It compared the thermal stability and glass transition temperature of several similar polymeric NPs that their data is presented in Table 4. As shown in the table, the thermal stability and glass transition temperature of the nanocomposite prepared by us are better than the reported ones. The polymeric NCs with superparamagnetic properties were also prepared by the addition of NiO NPs.

3.8 VSM analysis

The magnetization measurements of bare NiO NPs and PSt/NiO NCs were recorded at room temperature is shown in Fig. 8. As can be seen in Fig. 8a, the shape of the hysteresis loop is characteristic of superparamagnetic behavior (weak ferromagnetic) although bulk NiO is antiferromagnetic [53, 54]. From Fig. 8a, the coercive field (H_c) and the remnant magnetization (M_r) are estimated to be only 45.7 Oe and 0.0068 emu/g for NiO NPs. The maximum field applied, 8425 Oe does not saturate the magnetization (M_s) and the

Table 4 The thermal stability and glass transition temperature of several similar polymeric NCs

Polymeric NCs	Amount of NPs bonded to polymer (%)	Synthetic method for polymerization	Increased glass transition (°C)	Increased thermal stability (°C)	References
PSt/Fe_3O_4	6	Solvent	2.2	–	[52]
PSt/SiO_2	5	Miniemulsion	4	10	[51]
PSt/Hg	4	Solvent	20	12	[10]
PSt/NiO	5	Miniemulsion	32	45	This work
PMMA/NiO	5	Suspension	10	30	[25]
PMMA/NiO	5	In situ bulk	–	35	[3]

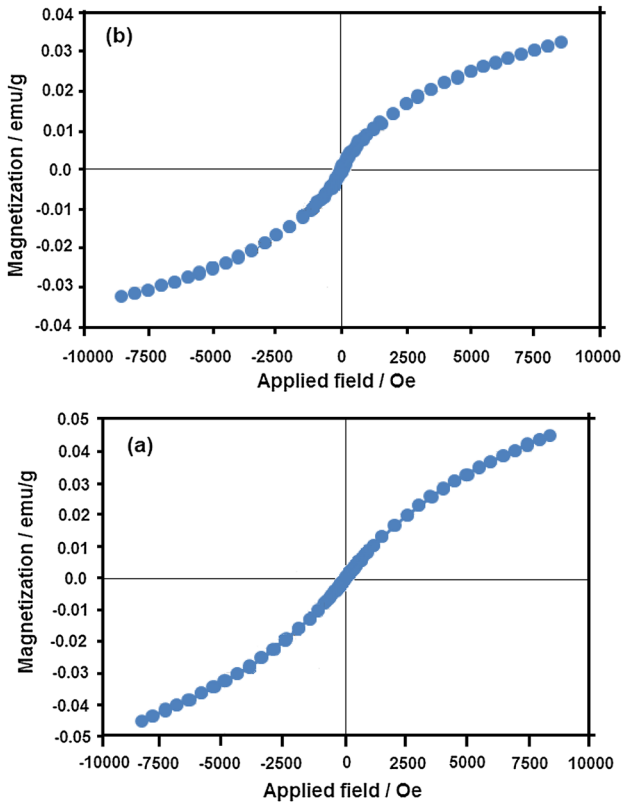

Fig. 8 Magnetization versus applied magnetic field at room temperature for: (**a**) bare NiO NPs and (**b**) PSt/NiO NCs

magnetization at this applied field is 0.45 emu/g. The low coercive field and remnant magnetization confirm that NiO NPs exhibit a little ferromagnetic property. The non-saturation of the magnetization is characteristic of superparamagnetic (weak ferromagnetic) ordering of the spins in the NPs. NiO NPs is made of small magnetic domains. Each magnetic domain is characterized by its own magnetic moment oriented randomly. The total magnetic moment of the NPs is the sum of these magnetic domains coupled by dipolar interactions [55, 56]. As a result, a low value of remnant magnetization is obtained. The magnetic properties of NPs

Table 5 Magnetic parameters of NiO NPs and polymer/NiO NCs

Material	Coercive field (Oe)	Magnetic saturation (emu/g)	Remnant magnetization (emu/g)	References
NiO NPs	66	0.065	0.002	[57]
NiO NPs	452	1.19	0.098	[58]
NiO NPs	45.7	0.45	0.0068	This work
NiO NPs	334.5	0.226	0.0046	[59]
PANI/NiO NCs	238	0.45	0.040	[58]
PSt/NiO NCs	49.0	0.033	0.0032	This work
EDTA/NiO NCs	279	0.232	0.0047	[59]

have been believed to be highly dependent on the sample shape, crystallinity, magnetization direction.

As can be seen in Fig. 8b, the coercive field (H_c) and the remnant magnetization (M_r) are estimated to be only 49 Oe and 0.0032 emu/g for PSt/NiO NCs. The maximum field applied, 8460 Oe does not saturate the magnetization (M_s) and the magnetization at this applied field is 0.033 emu/g. The addition of polymer to nanoparticles causes its magnetism to be reduced. But more importantly, with the addition of NiO NPs to a polymer such as polystyrene, a polymer nanocomposite is obtained with paramagnetic character.

It compared the magnetization measurements of several similar NiO NPs and polymeric NCs containing NiO NPs that their data is presented in Table 5. As shown in the table, magnetic saturation and coercive field of the PSt/NiO NCs prepared by us are lower than the reported ones.

4 Conclusions

NiO_2 was prepared from reaction of $Ni(NO_3)_2{\cdot}6H_2O$ with sodium hypochlorite in the present of CTAB in alkaline solution, and then its oxidation by ethanol, obtained NiO nanoparticles (NPs). PSt/NiO NCs were prepared via in situ miniemulsion polymerization from the reaction of polystyrene and modified NiO NPs by APS as radical initiator. The

NiO NPs and PSt/NiO NCs prepared by our method are simpler and less costly as well as smaller particles with lower calcining temperature. The surface of NiO NPs was changed to the hydrophobic character due to surface modification using oleic acid and grafted by polystyrene. The results showed that LD of modified NiO NPs increased with the rising amount of modifier up to 5% wt. Optimum modification was obtained at 65 °C and 4 h for reaction time. The XRD pattern showed embedded polystyrene to NiO NPs reduced crystallinity of NPs, so that the height and intensity peak of NCs is reduced. FTIR spectra revealed a single molecular layer is composed of oleic acid on the surface of NiO NPs. SEM showed that PSt/NiO NCs are completely spherical particles and like dandelion flower. The NCs were well distributed in the matrix and produce excellent monodispersion. The TGA and DSC analysis showed that the NCs contain 5% wt NiO NPs, and the thermal stability of polymer increased about 30 °C and its glass transition temperature increased about 10 °C due to incorporation of NiO NPs into PSt polymer. The NiO NPs have paramagnetic behavior. The polymeric NCs with superparamagnetic properties were also prepared by the addition of NiO NPs.

Acknowledgements The authors would like to thank the Research Council of Shahrood University of Technology for the financial support of this work.

Compliance with ethical standards

Conflict of interest The authors declare that they have no conflict of interest.

References

1. J.J. Luo, I.M. Daniel, Characterization and modeling of mechanical behavior of polymer/clay nanocomposites. Compos. Sci. Technol. **63**, 1607–1616 (2003)
2. A.R. Mahdavian, M. Ashjari, A.B. Makoo, Preparation of poly(styrene-methyl methacrylate)/SiO_2 composite nanoparticles via emulsion polymerization: An investigation into the compatiblization. Eur. Polym. J. **43**, 336–344 (2007)
3. L.A. Garcıa-Cerda, L.E. Romo-Mendoza, M.A. Quevedo-Lopez, Synthesis and characterization of NiO nanoparticles and their PMMA nanocomposites obtained by in situ bulk polymerization. J. Mater. Sci. **44**, 4553–4556 (2009)
4. H.R. Kricheldorf, O. Nuyken, G. Swift, *Handbook of Polymer Synthesis*, 2nd edn. (Marcel Dekker, New York, 2005), pp. 77–78
5. Á Costoyas, J. Ramos, J. Forcada, Encapsulation of silica nanoparticles by miniemulsion polymerization. J. Polym. Sci. A **47**, 935–948 (2009)
6. Y. Wang, H. Xu, H. Gu, Synthesis of raspberry-like SiO_2/polystyrene nanocomposite particles via miniemulsion polymerization. J. Nanosci. Nanotechnol. **9**, 1571–1576 (2009)
7. S.-W. Zhang, S. Zhou, Y.-M. Weng, L.-M. Wu, Synthesis of SiO_2/polystyrene nanocomposite particles via miniemulsion polymerization. Langmuir **21**, 2124–2128 (2005)
8. F. Yan, J. Li, J. Zhang, F. Liu, W. Yang, Preparation of Fe_3O_4/polystyrene composite particles from monolayer oleic acid modified Fe_3O_4 nanoparticles via miniemulsion polymerization. J. Nanopart. Res. **11**, 289–296 (2009)
9. L.P. Ramírez, K. Landfester, Magnetic polystyrene nanoparticles with a high magnetite content obtained by miniemulsion processes. Macromol. Chem. Phys. **204**, 22–31 (2003)
10. P.S. Nair, T. Radhakrishnan, N. Revaprasadu, C.G.C.E. van Sittert, V. Djokovic, A.S. Luyt, Characterization of polystyrene filled with HgS nanoparticles. Mater. Lett. **58**, 361–364 (2004)
11. X.L. Sun, Z.P. Fan, L.D. Zhang, L. Wang, Z.J. Wei, X.Q. Wang, W.L. Liu, Superhydrophobicity of silica nanoparticles modified with polystyrene. Appl. Surf. Sci. **257**, 2308–2312 (2011)
12. B. Kaboudin, H. Khanmohammadi, F. Kazemi, Polymer supported gold nanoparticles: synthesis and characterization of functionalized polystyrene-supported gold nanoparticles and their application in catalytic oxidation of alcohols in water. Appl. Surf. Sci. **425**, 400–406 (2017)
13. C. Hodges, Y. Ding, S. Biggs, The influence of nanoparticles on polystyrene adhesion. Adv. Powder Technol. **21**, 13–18 (2010)
14. K. Tian, C. Liu, H. Yang, X. Ren, In situ synthesis of copper nanoparticles/polystyrene composite. Colloids Surf. A **397**, 12–15
15. J. Chen, G. Cheng, Y. Chai, W. Han, W. Zong, J. Chen, C. Li, W. Wang, L. Ou, Y. Yu, Preparation of nano-$CaCO_3$/polystyrene nanocomposite beads for efficient bilirubin removal. Colloids Surf. B **161**, 480–487 (2018)
16. W. Han, Y. Bai, S. Liu, C. Ge, L. Wang, Z. Ma, Y. Yang, X. Zhang, Enhanced thermal conductivity of commercial polystyrene filled with core-shell structured BN@PS. Composites A **102**, 218–227 (2017)
17. O. Bera, B. Pilic, J. Pavlicevic, M. Jovicic, B. Hollo, K.M. Szecsenyi, M. Spirkova, Preparation and thermal properties of polystyrene/silica nanocomposites. Thermochim. Acta **515**, 1–5 (2011)
18. J. Gu, N. Li, L. Tian, Z. Lv, Q. Zhang, High thermal conductivity graphite nanoplatelet/UHMWPE nanocomposites. RSC Adv. **5**, 36334–36339 (2015)
19. J. Gu, Y. Guo, X. Yang, C. Liang, W. Geng, L. Tang, N. Li, Q. Zhang, Synergistic improvement of thermal conductivities of polyphenylene sulfide composites filled with boron nitride hybrid fillers. Composites A **95**, 267–273 (2017)
20. X. Yang, L. Tang, Y. Guo, C. Liang, Q. Zhang, K. Kou, J. Gu, Improvement of thermal conductivities for PPS dielectric nanocomposites via incorporating NH_2-POSS functionali-zed *n*BN fillers. Composites A **101**, 237–242 (2017)
21. Y. Guo, G. Xu, X. Yang, K. Ruan, T. Ma, Q. Zhang, J. Gua, Y. Wu, H. Liud, Z. Guo, Significantly enhanced and precisely modeled thermal conductivity in polyimide nanocomposites by chemically modified graphene via in-situ polymerization and electrospinning-hot press technology. J. Mater. Chem. C (2018). https://doi.org/10.1039/C8TC00452H
22. E. Soleimani, R. Taheri, Synthesis and surface modification of CuO nanoparticles: Evaluation of dispersion and lipophilic properties of modified nanoparticles. Nano-Struct. Nano-Object. **10**, 167–175 (2017)
23. J.-H. Kang, Y.-P. Guo, Y. Chen, Z.-C. Wang, Preparation and UV-light absorption property of oleic acid surface modified ZnO nanoparticles. Chem. Res. Chin. Univ. **27**, 500–502 (2011)
24. R.Y. Hong, L.L. Chin, J.H. Li, H.Z. Li, Y. Zheng, J. Ding, Preparation and application of polystyrene-grafted ZnO nanoparticles. Polym. Adv. Technol. **18**, 901–906 (2007)
25. E. Soleimani, F. Babaei-Niavarzi, Preparation, characterization and properties of PMMA/NiO polymer nanocomposites. J. Mater. Sci.: Mater. Electron. **29**, 2392–2405 (2018)
26. F.A. Harraz, R.M. Mohamed, A. Shawky, I.A. Ibrahim, Composition and phase control of Ni/NiO nanoparticles for photocatalytic degradation of EDTA. J. Alloys Compd. **508**, 133–140 (2010)

27. D.Y. Han, H.Y. Yang, C.B. Shen, X. Zhou, F.H. Wang, Synthesis and size control of NiO nanoparticles by water-in-oil microemulsion. Powder Technol. **147**, 113–116 (2004)
28. X. Guo, L. Zhao, L. Zhang, J. Li, Surface modification of magnesium aluminum hydroxide nanoparticles with poly(methylmethacrylate) via one-pot in situ polymerization. Appl. Surf. Sci. **258**, 2404–2409 (2012)
29. Y. Chung, S.R. Yun, C.W. Lee, N.J. Jo, C.H. Yo, K.S. Rya, Inorganic/organic nanocomposites of polyaniline and Fe_3O_4 with hollow cluster structures using polystyrene template. Bull. Korean Chem. Soc. **31**, 2065–2068 (2010)
30. L. Feng, L. He, Y. Ma, Y. Wang, Grafting poly(methylmethacrylate) onto silica nanoparticle surfaces via a facile esterification reaction. Mater. Chem. Phys. **116**, 158–163 (2009)
31. M. Dadkhah, F. Ansari, M. Salavati-Niasari, Thermal treatment synthesis of SnO_2 nanoparticles and investigation of its light harvesting application. Appl. Phys. A **122**, 700 (2016)
32. M. Mahdiani, A. Sobhani, F. Ansari, M. Salavati-Niasari, Lead hexaferrite nanostructures: Green amino acid sol-gel autocombustion synthesis, characterization and considering magnetic property. J. Mater. Sci.: Mater. Electron. **28**, 17627–17634 (2017)
33. A. Khansari, M. Enhessari, M. Salavati-Niasari, Synthesis and characterization of nickel oxide nanoparticles from Ni(salen) as precursor. J. Clust. Sci. **24**, 289–297 (2013)
34. M.M. Kashani-Motlagh, A.A. Youzbashi, L. Sabaghzadeh, Synthesis and characterization of nickel hydroxide/oxide nanoparticles by the complexation-precipitation method. Int. J. Phys. Sci. **6**, 1471–1476 (2011)
35. C.B. Wang, G.Y. Gau, S.J. Gau, C.W. Tang, J.L. Bi, Preparation and characterization of nanosized nickel oxide. Catal. Lett. **101**, 241–247 (2005)
36. Y. Wang, W. Eli, L. Zhang, H. Gao, Y. Liu, P. Li, A new method for surface modification of nano-$CaCO_3$ and nano-Al_2O_3 at room temperature. Adv. Powder Technol. **21**, 203–205 (2010)
37. F. Ansari, M. Bazarganipour, M. Salavati–Niasari, $NiTiO_3$/$NiFe_2O_4$ nanocomposites: Simple sol–gel auto-combustion synthesis and characterization by utilizing onion extract as a novel fuel and green capping agent. Mater. Sci. Semicond. Proc. **43**, 34–40 (2016)
38. R. Ramos-González, L.A. García-Cerda, M.A. Quevedo-López, Study of the surface modification with oleic acid of nanosized HfO_2 synthesized by the polymerized complex derived sol–gel method. Appl. Surf. Sci. **258**, 6034–6039 (2012)
39. S.Y. Lee, M.T. Harris, Surface modification of magnetic nanoparticles capped by oleic acids: Characterization and colloidal stability in polar solvents. J. Colloid Interface Sci. **293**, 401–408 (2006)
40. R. Hong, T. Pan, J. Qian, H. Li, Synthesis and surface modification of ZnO nanoparticles. Chem. Eng. J. **119**, 71–81 (2006)
41. T.K. Jain, M.A. Morales, S.K. Sahoo, D.L. Leslie-Pelecky, V. Labhasetwar, Iron oxide nanoparticles for sustained delivery of anticancer agents. Mol. Pharm. **2**, 194–205 (2005)
42. S. Yang, H. Liu, Z. Zhang, Fabrication of novel multi hollow super paramagnetic magnetite/polystyrene nanocomposite microspheres via water-in-oil-in-water double emulsions. Langmuir **24**, 10395–10401 (2008)
43. X. Yan, Q. He, X. Zhang, H. Gu, H. Chen, Q. Wang, L. Sun, S. Wei, Z. Guo, Magnetic polystyrene nanocomposites reinforced with magnetite nanoparticles. Macromol. Mater. Eng. **299**, 485–494 (2014)
44. B. Faure, G. Salazar-Alvarez, A. Ahniyaz, I. Villaluenga, G. Berriozabal, Y.R. De Miguel, L. Bergström, Dispersion and surface functionalization of oxide nanoparticles for transparent photocatalytic and UV-protecting coatings and sunscreens. Sci. Technol. Adv. Mater. **14**, 023001 (2013)
45. A.A. Keller, H. Wang, D. Zhou, H.S. Lenihan, G. Cherr, B.J. Cardinale, R. Miller, Z. Ji, Stability and aggregation of metal oxide nanoparticles in natural aqueous matrices. Environ. Sci. Technol. **44**, 1962–1967 (2010)
46. S. Mallakpour, M. Madani, A review of current coupling agents for modification of metal oxide nanoparticles. Prog. Org. Coat. **86**, 194–207 (2015)
47. M. Salavati-Niasari, F. Mohandes, F. Davar, M. Mazaheri, M. Monemzadeh, N. Yavarinia, Preparation of NiO nanoparticles from metal-organic frameworks via a solid-state decomposition route. Inorg. Chim. Acta **362**, 3691–3697 (2009)
48. N. Tomczak, Sh. Gu, M. Han, N.F. Van Hulst, G.J. Vancso, Single light emitters in electrospun polymer nanofibers: Effect of local confinement on radioactive decay. Eur. Polym. J. **42**, 2205–2210 (2006)
49. L. Tang, B. Zhou, Y. Tian, H. Bala, Y. Pan, S. Ren, Y. Wang, X. Lv, M. Li, Z. Wang, Preparation and surface modification of uniform ZnO nanorods via an one-step process. Colloids Surf. A **296**, 92–96 (2007)
50. P. Liu, Z. Su, Preparation and characterization of PMMA/ZnO nanocomposites via in–situ polymerization method. J. Macromol. Sci. B **45**, 131—138 (2006)
51. A.S. Patole, S.P. Patole, M.H. Song, J.Y. Yoon, J.H. Kim, T.H. Kim, Synthesis and characterization of silica/polystyrene composite nanoparticles by in situ mini-emulsion polymerization. Elastom. Compos. **44**, 34–40 (2009)
52. P. Dallas, V. Georgakilas, D. Niarchos, P. Komninou, T. Kehagias, D. Petridis, Synthesis, characterization and thermal properties of polymer/magnetite nanocomposites. Nanotechnology **17**, 2046–2053 (2006)
53. F. Davar, Z. Fereshteh, M. Salavati-Niasari, Nanoparticles Ni and NiO: Synthesis, characterization and magnetic properties. J. Alloys Compd. **476**, 797–801 (2009)
54. M. Salavati-Niasari, N. Mir, F. Davar, Synthesis and characterization of NiO nanoclusters via thermal decomposition. Polyhedron **28**, 1111–1114 (2009)
55. Z. Fereshteh, M. Salavati-Niasari, K. Saberyan, S.M. Hosseinpour-Mashkani, F. Tavakoli, Synthesis of nickel oxide nanoparticles from thermal decomposition of a new precursor. J. Clust. Sci. **23**, 577–583 (2012)
56. M. Salavati-Niasar, F. Davar, Z. Fereshteh, Synthesis of nickel and nickel oxide nanoparticles via heat-treatment of simple octanoate precursor. J. Alloys Compd. **494**, 410–414 (2010)
57. S. Farhadi, Z. Roustaei-Zaniyani, Simple and low-temperature synthesis of NiO nanoparticles through solid-state thermal decomposition of the hexa(ammine)Ni(II)nitrate, $[Ni(NH_3)_6](NO_3)_2$, complex. Polyhedron **30**, 1244–1249 (2011)
58. B.I. Nandapure, S.B. Kondawar, M.Y. Salunkhe, A.I. Nandapure, Magnetic and transport properties of conducting polyaniline/nickel oxide nanocomposites. Adv. Mater. Lett. **4**, 134–140 (2013)
59. H.T. Rahal, R. Awad, A.M. Abdel–Gaber, D. El-Said Bakeer, Synthesis, characterization, and magnetic properties of pure and EDTA–capped NiO nanosized particles. J. Nanomater. **2017**, 7460323 (2017)